Since January 2020 Elsevier has created a COVID-19 resource centre with free information in English and Mandarin on the novel coronavirus COVID-19. The COVID-19 resource centre is hosted on Elsevier Connect, the company's public news and information website.

Journal of Hepatology, 1991; 13: 61–70
Elsevier Science Publishers B.V. 0168-8278/91/$03.50 © 1991

HEPAT 00852

Altered pathogenicity in the liver induced by a mouse hepatitis virus type 3 thermosensitive mutant

Jean-Pierre Martin, Annick Bingen, Françoise Koehren, Jean-Pierre Gut and André Kirn
Laboratoire de Virologie de la Faculté de Médecine et Unité de Recherches, INSERM U74, Strasbourg, France

(Received 11 July 1990)

Intraperitoneal inoculation into sensitive BALB/c mice of D85, a thermosensitive (ts) mutant, provokes acute hepatitis followed by recovery of the mice. The ts mutant was able to replicate in the liver. However, the maximal viral titre was obtained 2 days later than was the case with the wild-type (wt) MHV 3 infection; the viral antigens remained localized within small foci and no invasion of the entire liver was observed. The hepatocytes infected with D85 showed strong steatosis similar to that induced by wt virus, but the other lesions induced by MHV 3 (closing of endothelial cell fenestrae and hepatocytolysis) were not seen. An important feature noticed with the D85 mutant concerned the establishment, in the surviving animals, of persistent infection: this phenomenon was demonstrated by the decrease of viral titre in the liver, viral RNA detection, and the fact that viral antigens gradually decreased until the 3rd month post-infection.

Mouse hepatitis viruses (MHV) are enveloped viruses containing a single-stranded positive RNA genome. The viral RNA encodes three structural polypeptides: the phosphonucleoprotein N (60 kDa), the matrix glycoprotein M (21 kDa) and the glycoprotein of the peplomer S (180–90 kDa) responsible for attachment to receptors on permissive cells and for cell fusion. MHV produces a wide spectrum of diseases dependent on the particular viral strain as well as on host factors such as genetic background, age, route of infection and immune status (1–3). The MHV 3 strain causes acute hepatitis in most sensitive inbred mice including BALB/c mice (4). In this case, the infection of the Kupffer cells and endothelial cells is a prerequisite to the infection of the parenchymal cells in MHV 3 induced hepatitis (5–7). In vitro, all liver cells (Kupffer cells, endothelial cells (8) and hepatocytes (9)), are highly susceptible to MHV 3 which rapidly induces large syncytia in them. In the case of susceptible mice, infection by MHV 3 leads to the appearance of procoagulant activity induced by monocytes/macrophages and controlled by T lymphocytes resulting in abnormalities of microcirculation and the formation of sinusoidal microthrombi (10–13). We have recently isolated a panel of MHV 3 thermosensitive (ts) mutants to study the viral factors involved in the hepatitis induced in sensitive BALB/c mice (14). This paper describes the pathogenicity of one mutant: D85. The replication of this mutant is reduced only at a temperature above 38 °C. At 37 °C, D85 is able to replicate in DBT cells. Biochemical studies showed that it was an RNA positive mutant. No difference was observed in the size of the viral intracellular RNA species or in the molecular weight of viral proteins.

Materials and Methods

Cells and viruses

Mouse L 2 cells and DBT cells were grown separately in a minimum essential medium (MEM) containing 10% fetal calf serum. The wild-type (wt) MHV 3 strain and the ts

Correspondence: J.-P. Martin, Laboratoire de Virologie, rue Koeberlé, 67000 Strasbourg, France.

mutant used in this study have been previously described (14).

Animals

Ten week-old BALB/c mice were inoculated intraperitoneally (i.p.) with $1 \cdot 10^3$ PFU of wt virus or ts mutant. Mice were killed at various times post infection (p.i.) and blood and livers were collected. The livers were immediately frozen in liquid nitrogen and stored at −80 °C; blood was allowed to clot for 1 h at 37 °C and the serum was collected and stored at −20 °C prior to assay.

Virus titration in the liver

Chilled pieces of liver were homogenized twice for 15 s in PBS buffer (5 ml/g of liver) with a Politron homogenizer. The virus titre was determined by plaque assays on L 2 cells, as previously described (14).

RNA extraction and hybridization

RNA was isolated from 0.3 g of liver from uninfected, MHV 3 infected, and D85 infected mice at different times using the guanidine isothiocyanate method (15). For blot analysis, RNA in NTE (0.01 M Tris-HCl (pH 7.4), 0.1 M NaCl, 1 mM EDTA) was applied to nitrocellulose filters. Prehybridization was performed in 10× SSC (1× SSC is 0.15 M NaCl, 0.015 M sodium citrate), 10% formaldehyde, 5× Denhardt's solution (50× Denhardt's solution is 1% bovine serum albumine, 1% Ficoll and 1% polyvinylpyrrolidone) at 60 °C. Hybridization was performed in the same solution with the addition of $1 \cdot 10^6$ cpm/ml of [^{32}P]cDNA from the purified denatured genomic RNA of MHV 3. Filters were washed four times at room temperature in 2× SSC and 0.2% SDS, twice in 2× SSC, 0.1% SDS at 55 °C and exposed to Curix film (Agfa Gevaert) at −80 °C.

Indirect immunofluorescence assay (IFA)

Frozen sections (1 μm) of liver were cut on a cryostat before being used for indirect immunofluorescent or histological studies. The sections were fixed for 10 min with acetone and washed twice for 5 min in PBS. Anti-MHV 3 antibody (100 μl/section) was absorbed for 30 min at room temperature. Sections were then washed three times in PBS. Fluorescein-labeled anti-mouse immunoglobin G (100 μl/section) (Institut Pasteur Production) was added for 30 min at room temperature. Each slide was washed three times in PBS overlaid with glycerol (PBS/glycerol, 9:1) and examined under a Leitz fluorescent microscope. Anti-MHV 3 antibody was produced in the resistant A/J mice strain by two i.p. injections of $1 \cdot 10^3$ PFU/mouse; for most experiments the antibody was used at a final dilution of 1:100.

Electron microscopy

TEM: Mouse livers were fixed by perfusion with 1.5% glutaraldehyde buffered with 75 mM cacodylate at pH 7.4 through the portal vein according to the method of Wisse (16). Small blocks were post-fixed in phosphate-buffered 1% OsO_4 for 1 h and dehydrated with ethanol. Epon was used as an embedding medium and thin sections stained with uranyl acetate and lead citrate were observed under a Philips EM 410 electron microscope (Eindhoven, The Netherlands).

To determine the extent and localization of the lesions, 1 μm semi-thin sections from the same samples used for TEM were stained with toluidine blue and observed under a light microscope.

Freeze-fracture

The perfused livers, cut into very small blocks, were fixed for 30 min more with 2% glutaraldehyde either in a phosphate buffer (pH 7.4) or in a 0.1 M cacodylate buffer containing 1 mM $MgCl_2$, 1 mM $CaCl_2$ and 4.5% sucrose (pH 7.3). They were then washed and glycerinated in 30% glycerol in the corresponding buffer for at least 4 h at 4 °C. Each block, placed inside a suitable copper specimen holder (Balzers), was frozen in subcooled nitrogen (close to −210 °C). The frozen specimens were then fractured either immediately or after a period of storage under liquid nitrogen in a Reichert-Jung 190 cryofract freeze-fracture device at −150 °C (Cambridge Instruments, Villepinte, France). The fracture planes were replicated with platinum at 45° and coated with carbon. The replicas were cleaned in sodium hypochloride, washed in three changes of distilled water and picked up on hexagonal 700 mesh gold grids. They were examined in a Philips EM 410 electron microscope. Morphometry was performed on electron micrographs with a Kontron semiautomatic MOP Videoplan analyzer (Eching/Munich, F.R.G.). About 4000 μm^2 of endothelial cell membranes from untreated liver or from mice liver inoculated with MHV 3 were examined.

SEM

After the same fixation and dehydration processes used for TEM, the liver samples were dried in a critical point dryer, coated with gold and observed under a Philips SEM 501 electron microscope.

Results

In vitro multiplication

At 37 °C, the wt virus and the ts mutant D85 replicate equally well in DBT cells (Fig. 1A). However, at the per-

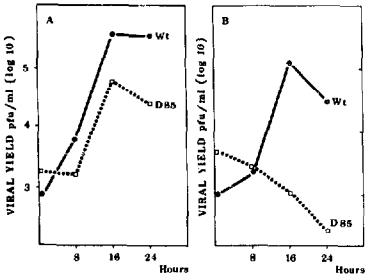

Fig. 1. Kinetics of virus multiplication at 37 °C (A) and 39.5 °C (B). DBT cells were infected with wt or ts mutant at 0.1 PFU/cell. At various times p.i. samples were taken for virus titration on L 2 cells.

missive temperature, the maximum titre obtained with the ts mutant was approx. 10-times lower than that of the wt virus. At 39.5 °C, the replication of D85 was completely inhibited (Fig. 1B).

Clinical signs and effects of ts mutant

To compare the pathogenicity of D85 to wt MHV 3, groups of twenty mice were inoculated i.p. with $1 \cdot 10^3$ PFU/mouse. This route was chosen because it had been demonstrated to result in earlier death of sensitive animals. Whilst wt MHV 3 killed 100% of the mice at 5 days p.i., D85 only killed 15% of the mice during the same period (Fig. 2A). Although the LD_{50} of wt MHV 3 was less than 1 PFU/mouse, inoculation of as much as $5 \cdot 10^4$ PFU/mouse of D85 only killed 35% of the mice. Daily inspection showed that both groups of mice exhibited general lethargy. This symptom initially appeared 1.5 to 2 days p.i. in the case of the wt virus and 3 days p.i. in that of the mutant, and persisted until death or recovery. The body temperature of the mice remained at the same level throughout the infection (data not shown) indicating that survival following infection with this mutant was not a result of an increase in body temperature.

Viral replication in the liver

Viral titres. Maximal virus titre in liver homogenates was the same with both viruses (Fig. 2B). However, the maximal titre for the D85 mutant occurred 1 to 2 days later than the equivalent point for the wt virus; this coincides with the maximum intensity of the clinical symptoms. During the recovery of D85 infected mice, the viral titre decreased rapidly and was undetectable after day 7. Virus isolated from the livers of D85 infected mice was

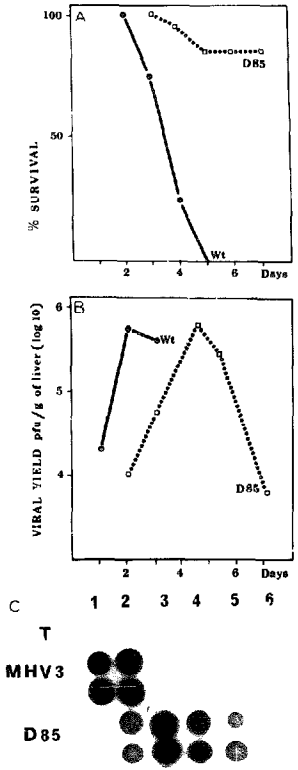

Fig. 2. (A) Curve of survival of 20 mice after i.p. inoculation with 10^3 PFU/mouse of wt virus or ts mutant. (B) Viral titres determined in the liver homogenates at different times post-infection with wt virus or ts mutant. (C) Dot blot hybridization of RNA from the liver of infected and uninfected (T) mice at different times (1–2 days, 2–3 days, 3–5 days, 4–10 days, 5–15 days, 6–45 days) with a cDNA probe from the entire genomic viral RNA.

still thermosensitive.

Viral RNA detection. RNA extracted from livers of two infected mice at different times p.i. was hybridized with a specific probe from genomic viral RNA. The dot blot analysis showed that the presence of MHV 3 RNA in the

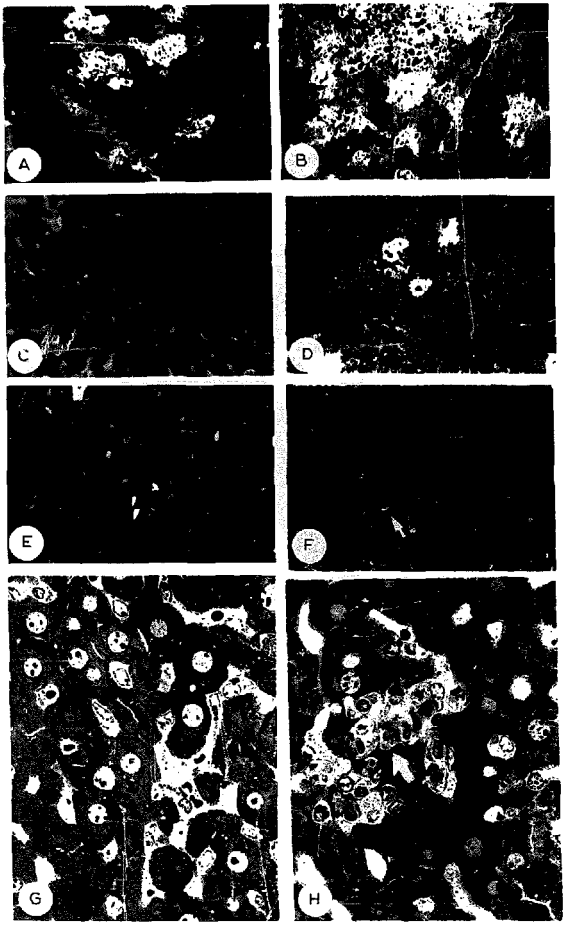

Fig. 3. Light microscopy: A–F indirect immunofluorescence performed on frozen liver sections. (A) Viral antigens of wt virus 2 days p.i. (B) 3 days p.i. (C) Uninfected liver. (D–F) Viral antigens of D85 respectively at 5 days (D), 10 days (E) and 3 months p.i. (F). The arrow points to the few hepatocytes stained with anti-MHV 3 (F). (G and H) Semi-thin sections/stained with toluidine blue. (G) Uninfected liver. ×560. (H) Mouse liver infected with wt virus for 52 h. Arrow indicates a necrotic area. ×560.

liver was maximal at 3 days p.i.; with D85 detection of viral RNA increased until 5 days p.i. and then decreased (Fig. 2C). The RNA could still be detected 20 days p.i., but from 45 days p.i. no RNA reacted with the probe. The probe did not bind to RNA isolated from uninfected mice livers.

Viral antigens. In frozen sections of liver, viral antigens could be detected by indirect immunofluorescence 24 h after intraperitoneal infection of wt virus. Antigens were prominent in the periportal areas and in sinusoidal cells. After 48 h, large amounts of viral antigens were localized in the hepatic parenchymal cells. The amount of antigen increased steadily until the death of the animals (Fig. 3A and B). In mice infected with mutant D85, viral antigens could be detected at 36 h p.i.; however, the foci remained of limited size for 5 days following infection (Fig. 3D) and then decreased until the 10th day (Fig. 3E). For up to 3 months p.i., antigens could still be detected in a very few individual cells (Fig. 3F). This suggests that after acute hepatitis, D85 induced a persistent infection

Light microscopy study

In control mice livers, hepatocytes presented round nuclei and the cytoplasm, rich in glycogen, contained few lipid droplets (Fig. 3G). From 48 h p.i. with wt virus, massive steatosis and numerous necrotic foci: picnotic nuclei and cytoplasmic lesions with accumulation of monuclear inflammatory cells were generally observed in the vicinity of the portal vein (Fig. 3H). With the D85 strain, necrotic areas were neither as numerous nor as extensive compared to those induced by the wt virus. The majority of the hepatocytes did not appear damaged apart from the areas of extensive steatosis (not shown).

Electron microscopy study

In the liver of control mice, observed at TEM level, the cytoplasm of the hepatocytes displayed a normal appearance: glycogen and mitochondria were numerous and few lipid droplets were visible. The sinusoid, devoid of red blood cells was lined by endothelial cells, in its lumen Kupffer cells were present (Fig. 4A). At the SEM level endothelial cells displayed numerous fenestrae arranged in sieve plates (Fig. 4B and insert). These were also visible on the E and P faces of the fracture of endothelial cell membranes (Fig. 4C). Three hundred and twenty-one fenestrae were counted in this figure for a surface of 37.5 μm^2 of endothelial cell membrane. After wt virus infection, sinusoidal lesions were evident at the TEM level (Fig. 5A). Sinusoids were invaded with red blood cells, plasma, cellular debris and fibrin deposits often associated with numerous viral particles (Fig. 5A, insert). Kupffer cells were no longer visible and the endothelial lining was sometimes interrupted. In addition, SEM examination revealed that when endothelial cells were present in the sinusoids invaded with red blood cells (Fig. 5B), they displayed only a few fenestrae (insert Fig. 5B) compared to uninfected liver endothelial cells (insert Fig. 4B). After freeze-fracture, TEM examination confirmed this surprising decrease in the number of endothelial cell fenestrae (Fig. 5C) which did not involve any other apparent cellular membrane lesions. In this figure only 46 fenestrae were counted for a surface of 32.5 μm^2. In order to quantify this phenomenon a morphometric study was carried out on 4000 μm^2 of endothelial cell membranes of both control and infected mice livers and these results are summarized in Table 1. A 2-fold decrease in the number of fenestrae per unit surface was found after 3 days of infection with MHV 3.

In addition to these sinusoidal lesions, an important hepatocytolysis was observed 72 h p.i. (Fig. 5A). Only a few parenchymal cells were still recognizable. They displayed an accumulation of lipid droplets (Fig. 5A), a dilatation of the RER cisternae and picnotic nuclei (not shown). Viral particles were sometimes encountered near the large RER but were most frequently observed at the hepatocyte-sinusoid border (not shown), or in sinusoids associated with fibrin deposits (Fig. 5A, insert).

After infection with D85, we were able to observe similar necrotic lesions in the sinusoid and in the hepatocytes. But these lesions were found only in a few areas. The only noticeable change in the hepatocytes, apart from glycogen depletion, consisted of a widespread steatosis observed both under TEM (Fig. 6A) and SEM (Fig. 6B). The majority of sinusoidal cells were intact and the endothelial cells exhibited as many fenestrae (Fig. 6B) as those observed in uninfected cells (Fig. 4B and insert).

TABLE 1

Morphometric study of the counting of endothelial cell fenestrae in control and in MHV 3-infected mouse livers

Samples		Surface observed (μm^2)	Number of fenestrae	Number of fenestrae (per μm^2)
Uninfected mouse livers	1	672	2613	3.9
	2	3061.5	16038	5.2
	3	352	1679	4.8
Mouse livers infected with MHV 3 (3 days)	1	1062	2777	2.6
	2	316.5	650	2.0
	3	2787	7706	2.6

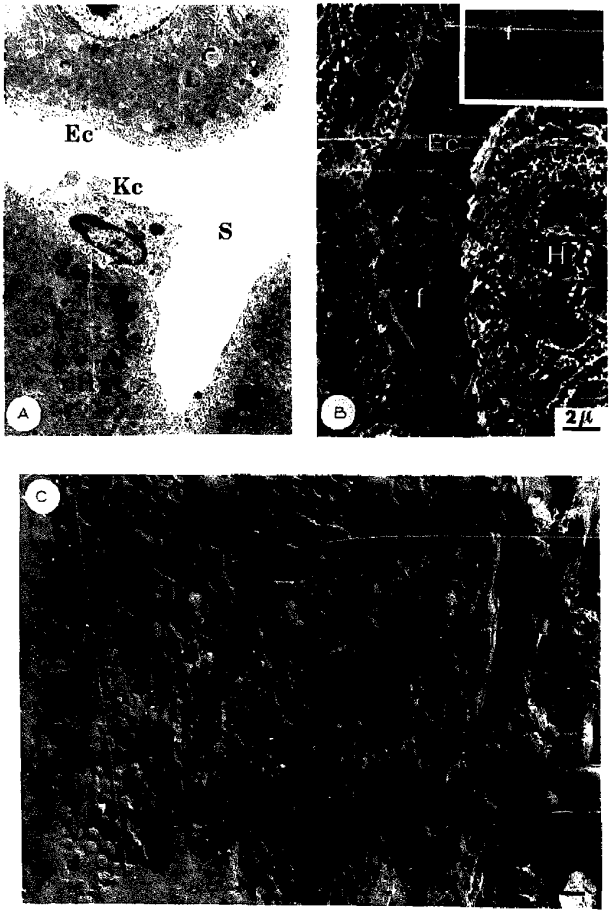

Fig. 4. Uninfected liver cells. (A) TEM. Ec, endothelial cell; Kc, Kupffer cell; S, sinusoid; H, hepatocyte; L, lipid inclusion. ×6800. (B) SEM. Ec, endothelial cell; H, hepatocyte; f, fenestrae. ×4300 and insert ×7300. (C) TEM after cryofracture. E, E face of the fracture; P, P face of the fracture; Ec, endothelial cell; H, hepatocyte; f, fenestrae. ×16 000.

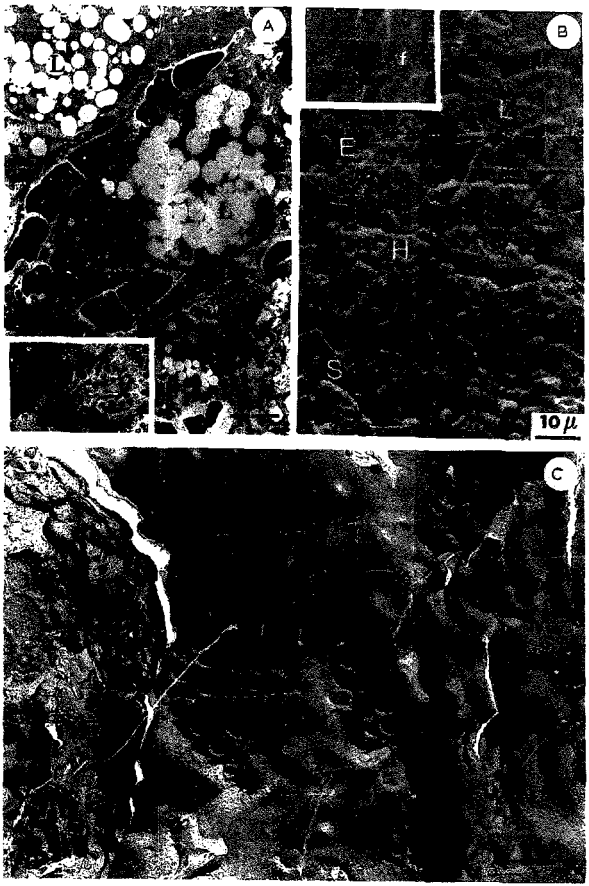

Fig. 5. Mice liver cells observed 3 days p.i. with wt virus. (A) TEM. The sinusoids (S) were invaded with erythrocytes (E), plasma and fibrin. Hepatocytes (H) filled with lipid inclusions (L) showed a necrotic area (arrow). ×2200. Insert: in sinusoids, MHV 3 particles (v) are often associated with fibrin deposits (f). ×20 500. (B) SEM. The hepatocytes (H) showed numerous cavities corresponding to lipid inclusions (L). The sinusoids (S) were filled with numerous erythrocytes (E). Endothelial cells displayed very few fenestrae (f) (insert). × 1070 and insert ×7500. (C) TEM after cryofracture. P face (P) of endothelial cells (Ec), lining and hepatocyte (H) displayed few fenestrae (f). A large surface of the endothelial cell membrane is devoid of fenestrae (*). ×16 000.

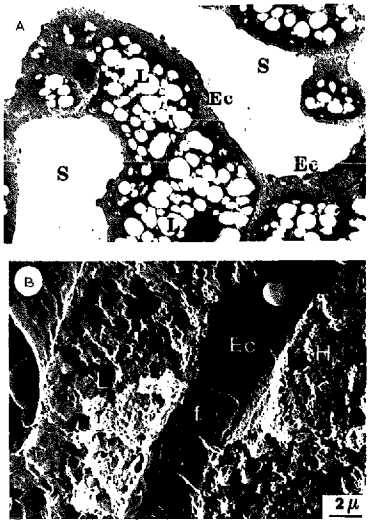

Fig. 6. Mouse livers observed 3 days after infection with D85 strain. (A) TEM. The sinusoids (S) were lined with uninterrupted endothelial cells (Ec). Beneath Ec an intact fat storing cell (FSC) could be observed. The hepatocytes contained many lipid inclusions (L). ×3500. (B) SEM. Endothelial cells (Ec) characterized by their fenestrae (f), as numerous as in untreated cells (5B), lined hepatocytes where numerous cavities previously filled with lipid droplets (L) could be observed. ×4500.

Discussion

Inoculation of wt MHV 3 into BALB/c mice produces a fulminating hepatitis which leads to the death of the animals in 3 or 4 days. This study reports the biological activities of a ts mutant and an attempt to correlate the severity of the disease with histological and ultrastructural observations. The ts mutant D85 was chosen since it is able to replicate in vitro at mouse body temperature (37.5 °C). D85 was clearly an attenuated virus strain since only about 15% of the mice died after i.p. inoculation of 1000 PFU. Histological observations of liver injury after wt virus infection was nearly identical to that previously reported with MHV 3 by Levy et al. (6). They also noticed the damage of the sinusoidal barrier, the presence of inflammatory foci and necrotic areas, and extensive intravascular coagulation. The only differences we observed in hepatocyte lesions were the significant modifications of the peroxysomes (17) and the accumulation of lipids in the liver, which seems specific to our virus strain. The origin of lipid accumulation in the liver is unknown, but biochemical determinations in the whole liver have shown an increase in the level of triglycerides and cholesterol (unpublished data).

Electron microscope observations confirmed that, after wt MHV 3 infection, the first lesions appeared in the hepatic sinusoid where the destruction of Kupffer cells and endothelial cells preceded the appearance of the hepatocyte lesions (7). We also observed a 2-fold decrease in the number of fenestrae in endothelial cells. For a morphometric study we used the freeze-fracture technique (the best method to study membranes). Similar findings have been obtained in vivo and in vitro after infection of isolated endothelial liver cells (18). The 'closing' of 50% of the fenestrae was probably the result of the fusion activity of the S glycoprotein incorporated into the cytoplasm membrane of the infected endothelial cells and could be explained by the disturbed fluidity of endothelial cell membranes in infected mice livers. Recent results have shown that the cholesterol content in these membranes was considerably decreased (19).

D85 infection induced a strong steatosis which was quite similar to that induced by wt MHV 3. This accumulation of lipids did not seem to be correlated with sinusoidal damages since it appeared in D85 infected mice which presented only few sinusoidal cell lesions and the majority of endothelial cell membranes showed normal fenestration.

An important feature of D85 infection was the establishment in the surviving animals of persistent infection: after the 7th day p.i., the virus titre was no longer detectable in the liver but the RNA could be detected 20 days p.i. and a very small number of hepatocytes with viral antigens could be observed after 1.5 months. The differences between non-infectious particle production, viral RNA, and protein detection could be explained by various factors: (i) differences in the sensibility of the three detection techniques; (ii) blockage of translation, since viral mRNAs seemed to be intact; (iii) selective degradation of viral mRNAs by host enzymes, while allowing remaining mRNAs to continue coding for proteins; and (iv) inhibition of viral maturation, either due to genomic mutations or to modification of glycosylation of S and M proteins and phosphorylation of N protein. At this stage, D85 infection appeared similar to the persistent infection of semi-sensitive C_3H mice infected with the wt MHV 3 (20).

The induction of a persistent infection is common to various viruses as well as to ts mutants (Sinbis Virus (21), Measles Virus (22), Vesicular Stomatitis Virus (23)). In

the case of Coronavirus infections, some ts MHV 4 or MHV A59 mutants are able to induce a chronic demyelinisating disease, whereas the wild-type provokes acute encephalitis (24–28).

The ability of D85 mutant to induce a persistent viral infection was probably the result of host factors. The delay in D85 multiplication could allow for a specific or non-specific immunological antiviral response which is able to inhibit viral replication. The factors involved could be T cells and macrophages which are the main elements of defense against MHV 3 infection (29). The ultrastructural observations showed that the sinusoidal cells were largely intact after D85 infection. In fact, Kupffer cells were able to play their protective role during D85 infection and endothelial cells were still able to maintain the exchange between hepatocytes and blood. The small inflammatory foci observed in the liver infected with this mutant could be due to the induction or regulation of immunological mediators (interleukin-1, tumor necrosis factor, and prostaglandins).

The persistent viral infection could also be due to the intrinsic properties of the D85 strain. In tissue cultures, D85 induced small plaques. In contrast, wt virus provoked large syncytia. This probably reflected an alteration of the fusion function provided by the S glycoprotein. The ts phenotype of D85 could reflect the preservation of the fenestrated areas in the endothelial cells. In this case, the endothelial cells role as filter was intact and could explain the modification of the disease.

Our study focused on the fact that a mutation in the *C* gene coding for S protein probably transformed lethal, fulminating hepatitis into a mild persistent infection. A similar mutation of MHV 4 transforms an acute encephalomyelitis to a subacute demyelinating disease (30–33). The ts D85 model may be helpful to further our understanding of host and viral factors implicated in acute and persistent disease. Our MHV 3 viral strains are a unique experimental model for viral induced steatosis in adult mice.

Acknowledgements

We wish to thank Michèle Valle for photographic work and technical assistance, Véronique Risch for typing the manuscript, Robert Drillien, Anne-Marie Aubertin and Georges Obert for helpful discussions and Liane Acito-Khan for the english adaptation of this manuscript. This research was supported by I.N.S.E.R.M. (Institut National de la Santé et de la Recherche Médicale) and a grant 87/901 from the D.R.E.T. (Direction des Recherches, Etudes et Techniques).

References

1 Tyrrell DAJ. Coronaviridae. Intervirology 1978; 10: 321–36.
2 Robb JS, Bond CW. Coronaviridae. In: Fraenkel-Conrat H, Wagner RR, eds. Comprehensive Virology. New York: Plenum Press, 1979; 14: 193–247.
3 Siddell SG, Wege H, Ter Meulen V. Biology of coronaviruses. J Gen Virol 1983; 64: 761–76.
4 Wege H, Siddell SG, Ter Meulen V. The biology and pathogenesis of coronaviruses. Curr Top Microbiol Immunol 1982; 99: 131–63.
5 Kirn A, Gut JP, Gendrault JL. Interaction of viruses with sinusoidal cells. Prog Liver Dis 1982; 3: 377–92.
6 Levy GA, Mac Phee PJ, Fung LS, Fisher MM, Rappaport AM. The effect of mouse hepatitis virus infection on the microcirculation of the liver. Hepatology 1983; 3: 964–73.
7 Steffan AM, Pereira CA, Kirn A. Role of the sinusoidal cells in the course of the hepatitis induced by mouse hepatitis type 3 (MHV 3) in mice. In: Kirn A, Knook DL, Wisse E, eds. Cells of the Hepatic Sinusoid. The Kupffer Cell Foundation: Rijswijk, 1986; 1: 377–8.
8 Pereira CA, Steffan AM, Kirn A. Interaction between mouse hepatitis viruses and primary cultures of Kupffer and endothelial liver cells from resistant and susceptible inbred mouse strains. J Gen Virol 1984; 65: 1617–20.
9 Arnheiter H, Baechi T, Haller O. Adult mouse hepatocytes in primary monolayer culture express genetic resistance to mouse hepatitis virus type 3. J Immunol 1982; 129: 1275–81.
10 Levy GA, Leibowitz JL, Edgington TS. Induction of monocyte procoagulant activity by murine hepatitis virus type 3 (MHV 3) parallels disease susceptibility in mice. J Exp Med 1981; 154: 1150–63.
11 Levy GA, Leibowitz JL, Edgington TS. Lymphocyte-instructed monocyte induction of the coagulation pathways parallels the induction of hepatitis by murine hepatitis virus. In: Popper H, Schaffner F, eds. Progress in Liver Disease, Vol. 7. New York: Grune and Stratton, 1982; 393–409.
12 Mac Phee PJ, Dindzans VI, Fung LS, Levy GA. Acute and chronic changes in the microcirculation in the inbred strains of mice following infection with mouse hepatitis virus type 3. Hepatology 1985; 5: 649–60.
13 Abecassis M, Falk J, Dindzans V, et al. Prostaglandin E2 prevents fulminant hepatitis and the induction of procoagulant activity in susceptible animals. Transplant Proc 1987; 19: 1103–5.
14 Martin JP, Koehren F, Rannou JJ, Kirn A. Temperature-sensitive mutants of mouse hepatitis virus type 3 (MHV 3). Isolation, biochemical and genetic characterization. Arch Virol 1988; 100: 147–60.
15 Maniatis T, Fritsch EF, Sambrook J. Molecular Cloning. A laboratory manual. New York: Cold Spring Harbor Laboratory Press, 1982.
16 Wisse E. An ultrastructural characterization of the endothelial cell in the rat liver sinusoid under normal and various experimental conditions, as a contribution to the distinction between endothelial and Kupffer cells. J Ultrastruct Res 1972; 38: 528–62.
17 De Craemer D, Bingen A, Langendries M, Martin JP, Roels F. Alterations of hepatocellular peroxisomes in viral hepatitis in the mouse. J Hepatol 1990; 11: 145–52.
18 Steffan AM, Gendrault JL, Kirn A. Phagocytosis and surface

modulation of fenestrated areas. Two properties of murine endothelial liver cells (EC) involving microfilaments. In: Kirn A, Knook DL, Wisse E, eds. Cells of the Hepatic Sinusoid. Rijswijk: The Kupffer Cell Foundation, 1986; 1: 483–8.
19 Bingen A, Martin JP, Kirn A. Decrease in the amount of filipin-cholesterol complexes in the membrane of liver endothelial cells after infection of mice with Mouse Hepatitis Virus 3 (MHV_3). An ultrastructural study. In: Wisse E, Knook DL, Mc Cuskey RS, eds. Cells of the Hepatic Sinusoid. Rijswijk: The Kupffer Cell Foundation, 1991, in press.
20 Le Prevost C, Virelizier JL, Dupuy JM. Immunopathology of mouse hepatitis virus type 3 infection III. Clinical and virologic observation of a persistent viral infection. J Immunol 1975; 115: 640–5.
21 Shenk TE, Kosbenyk KA, Stoller V. Temperature sensitive virus from acutes albopictus cells chronically infected with sindbis virus. J Virol 1974; 13: 439–47.
22 Lucas A, Coulter M, Anderson R, Flintoff V. In vivo and in vitro models of demyelinatory diseases: persistence and host-regulated thermosensitivity in cells of neural derivation infected with MHV and measles virus. Virology 1978; 88: 325–37.
23 Sekellick MJ, Marcus PI. Persistent infection. Interferon inducing temperature sensitive mutants as mediators of cell sparing. Possible role in persistent infections by VSV. Virology 1979; 95: 36–47.
24 Nagashima K, Wege H, Meyermann R, Ter Meulen V. Coronavirus induced subacute demyelinating encephalomyelitis in rat. Acta Neuropathol 1978; 44: 63–70.
25 Stohlman SA, Sakaguchi AY, Weiner LP. Characterization of the cold sensitive MHV mutants rescued from latently infected cells by cell fusion. Virology 1979; 98: 448–55.
26 Wege H, Watanabe R, Nagashima K, Ter Meulen V. Neurovirulence of MHV JHM temperature sensitive mutants in rats. Infect Immunol 1983; 39: 1316–26.
27 Ven Berlo MF, Wolswijk G, Calafat J, Koolen MJM, Horzineck MC, Von der Zeijst BAM. Restricted replication of MHV A59 in primary brain astrocytes correlates with reduced pathogenicity. J Virol 1986; 58: 426–33.
28 Lavi E, Gilden DH, Highkin MK, Weiss SR. Persistence of MHV A59 in a slow virus demyelinating infection in mice detected by in situ hybridization. J Virol 1984; 51: 563–6.
29 Stohlman SA, Frelinger JA, Weiner LP. Resistance to fatal central nervous system disease by mouse hepatitis virus strain JHM. II Adherent cell mediated protection. J Immunol 1980; 124: 1733–9.
30 Haspel MV, Lampert PW, Oldstone MBA. Temperature-sensitive mutants of mouse hepatitis virus produce a high incidence of demyelination. Proc Natl Acad Sci USA 1978; 75: 4033–6.
31 Knobler RL, Lampert PW, Oldstone MBA. Virus persistence and recurring demyelination produced by a temperature sensitive mutant of MHV 4. Nature (Lond.) 1982; 298: 279–80.
32 Fleming JO, Trousdale MD, El-Zaatari FAK, Stohlman SA, Weiner LP. Pathogenicity of antigenic variants of murine coronavirus JHM selected with monoclonal antibodies. Virology 1986; 58: 869–75.
33 Dalziel RG, Lampert PW, Talbot PJ, Buchmeier MJ. Site-specifique alteration of murine hepatitis virus type 4 peplomer glycoprotein E2 results in reduced neurovirulence. Virology 1986; 59: 462–71.